Computer Networks 52 (2008) 3101–3118

Contents lists available at ScienceDirect

Computer Networks

journal homepage: www.elsevier.com/locate/comnet

A multiple power-level approach for wireless sensor network positioning ☆

Jen-Yu Fang [a], Hung-Chi Chu [b,*], Rong-Hong Jan [a], Wuu Yang [a]

[a] Department of Computer Science, National Chiao Tung University, Hsinchu 30050, Taiwan
[b] Department of Information and Communication Engineering, Chaoyang University of Technology, Taichung County 41349, Taiwan

ARTICLE INFO

Article history:
Received 16 May 2007
Received in revised form 28 July 2008
Accepted 30 July 2008
Available online 14 August 2008

Responsible Editor: J.C. de Oliveira

Keywords:
Wireless sensor networks
Power-level
Positioning

ABSTRACT

Wireless sensor networks enhance our ability to monitor the physical world. Many recent researches on wireless sensor networks have focused on aspects such as routing, node cooperation, and energy consumption. In addition to these topics, the positioning service is also an important function in sensor networks. This paper presents a multiple power-level positioning algorithm, discusses its capabilities, and evaluates its performance in various environments. The simulation results show that the proposed algorithm exhibits better accuracy than do traditional single power-level methods. In critical situations such as reference node failure, unstable radio transmission range and beacon collision, the proposed algorithm still performs well. Finally, the positioning method is implemented on a sensor network test bed, and the actual measurements show that, the average estimation error is 2.5 m when three power-levels are used and adjacent reference nodes are 12 m apart in an outdoor environment.

1. Introduction

With the rapid progress of the wireless network technology, people can conveniently to communicate with one another any time and any place. Mobile devices with wireless capabilities have gradually been integrated into our daily life. A variant of the wireless networks is the wireless sensor network which integrates both wireless and sensor technology into a small device called a sensor node. Each sensor node has the ability to monitor the physical world and return the sensed information to control nodes via wireless communication.

Wireless sensor networks can be applied in many applications, such as military surveillance, environmental monitoring, health, home, and commerce [1]. Take a forest-fire detection system for example. A large number of sensor nodes are densely deployed in the forest. They are linked together with radio communication. Each sensor node relays both its location and the surrounding environmental information, such as: temperature, image, air pressure, wind speed, and so on, to the sink node. The sink node, which is a special sensor node, collects the sensed data and replies to the network manager. Abnormal sensed data will trigger a fire warning procedure. The locations of individual sensors are a necessary part of the sensed data since we want to know the precise location of a forest-fire when it occurs.

In radio communication, the location of a mobile node can be determined by several methods, such as angle of arrival (AOA) [2], time of arrival (TOA) [2], time difference of arrival (TDOA) [2], and received signal strength indicator (RSSI). These methods are based on telecommunications technology and need additional network equipment in order to determine a mobile node's location. In recent years, several positioning systems were proposed and implemented in real systems [3] such as global positioning system (GPS) [4], Active Badges [5], Active Bats [6], Cricket [7], RADAR [8], SpotOn [9] and so on. GPS is one of the most popular positioning systems for outdoor environment thus far. The average error of GPS is less than 3 m. However,

☆ This research was supported in part by the National Science Council, Taiwan, ROC, under grant NSC 96-2752-E-009-005-PAE, NSC 96-2219-E-009-006, and NSC 96-2219-E-009-008.

* Corresponding author. Fax: +886 4 23305539.
E-mail address: hcchu@cyut.edu.tw (H.-C. Chu).

1389-1286/$ - see front matter © 2008 Elsevier B.V. All rights reserved.
doi:10.1016/j.comnet.2008.07.013

these positioning methods are not suitable for wireless sensor networks due to size, cost, and power consumption constraints.

This paper aims at the scenario wherein a few reference nodes are deployed in static places, along with a lot more sensor nodes that can move around in the sensing field to collect data. A positioning method is developed using transmission signal overlapping region and multiple transmission power-levels. The transmission signal overlapping region of reference nodes was decided in the deployment stage. With the dense deployment in wireless sensor networks, the whole sensing field can be divided into independent regions. It should be noted that the independent region means the signal overlapping region that was formed by the set of different reference nodes. The independent region is helpful location information for narrowing down the possible location of a sensor node with geometric analysis. Furthermore, based on the power-levels of the transmission signal the whole sensing field can be divided into more and smaller independent regions. This improves the positioning accuracy. The proposed method is suitable for sensor networks that are constrained in terms of energy consumption, computation power, and device cost. This method also provides good location accuracy.

The remainder of this paper is organized as follows. The next section summarizes previous efforts in positioning research. Section 3 presents a distributed cell-based positioning method. The multiple power-level positioning approach and simulation results are presented in Sections 4 and 5, respectively. A hardware implementation of the proposed method is given in Section 6. Finally, a conclusion is given in Section 7.

2. Related works

As the wireless mobile device is in widespread use, it becomes more important in relation to a positioning demand for many wireless applications and services. There are many positioning methods in wireless networks, which can be classified into two classes: centralized positioning systems and distributed positioning systems. These positioning methods will be discussed in this section.

2.1. Centralized positioning systems

A centralized positioning system has a central server. The server collects the sensed data, accepts location queries, and sends replies back to the querying node. The location of a sensor node is obtained from the central server. Several mechanisms have been proposed for use in determining a node's location in a centralized positioning system. In AOA, TOA, and TDOA [2], additional devices are used in the network to determine the direction and the time (or time delay) of the signal, which are then used to calculate a node's location. Such solutions do not require modifications being made to mobile devices, but produce less accurate position estimates, and incur more network traffic. In an assisted GPS (AGPS) [10] system, an assistant server with a reference GPS receiver helps a handset with a partial GPS receiver to measure the range and estimate its position. The assistant server, which is a more powerful computing platform than a GPS receiver, has the ability to obtain information from the wireless channel. The assistant server communicates with a GPS receiver via a wireless channel to help the receiver quickly and efficiently estimate its location. In RADAR [8], a node converts the received signal strength (RSS) to distance information and uses a triangulation method to estimate a node's location. A convex positioning [11] system requires a central server to gather the connection information among all sensor nodes. The server uses the information to calculate a node's location. A cell-based positioning system [12] utilizes overlapped radio transmission signals of a transmitter to define several independent regions from the working area and a central location server to gather the information of independent regions and then estimates positions. Although these positioning methods produce acceptable position estimates, three major challenges still remain:

- *Time synchronization:* Because of central servers, nodes' locations could not be modified quickly when network topology changes.
- *Limited network bandwidth:* There are a limited number of usable channels. At any instant, only a few nodes can successfully transmit messages to the central server.
- *System instability:* All nodes' locations are determined by the central server. A broken communication link between a node and the central server would cause the positioning system to fail.

2.2. Distributed positioning systems

In a distributed positioning system, that is, one without a central server, every sensor node gathers the sensed data and uses a positioning algorithm to estimate its own location. GPS is a typical distributed positioning system [4]. It relies on 24 satellites that orbit around the earth and broadcast precise velocity, latitude, longitude, and altitude information. GPS produces more accurate location estimates but takes a longer time to first fix (TTFF) and incurs the additional cost of setting up a GPS receiver for each sensor node. One mechanism that does not rely on GPS measures the distances among the nodes to build a coordinated system by which relative positions of the nodes can be calculated [13]. Two area-based positioning mechanisms were also proposed [14,15]. One mechanism imposes the centroid of selected reference points to estimate its own position [14]. The other mechanism narrows down the possible region in which a particular node may reside. The region is formed by choosing three anchors from among all of the audible anchors and tests whether it is inside the triangle formed by these three anchors. The location of a node will be determined by the center of gravity of the intersection of triangles [15]. Niculescu and Nath introduced an ad hoc positioning system using GPS-like triangulation for estimating nodes' locations via distance-vector routing [16] or AOA [17] for range measurement. Based on multidimensional scaling (MDS), Shang et al. used the connectivity information to

derive the locations of the nodes [18]. In order to reduce the number of anchors, a few mobile anchors (equipped with the GPS capability) broadcast their current positions periodically [19]. Other sensor nodes that are deployed in static place use the receiving information to estimate their own locations. Note that our proposed method is based on static RNs and mobile SNs while the method in [19] is based on mobile anchors and static SNs. While all of the above distributed positioning systems produce acceptable location accuracy, there are still a number of defects:

- In GPS systems, not all sensor nodes can afford the GPS capability. Due to the limitations of sensor nodes in size, cost and power consumption, GPS receivers should be used sparingly.
- Owing to the limited computational power of sensor nodes, simpler positioning mechanisms are preferred to more complex ones.

3. Cell-based positioning method

A cell-based positioning system simply utilizes the characteristics of cell overlapping in geometry. It is noted that a *cell* is formed by a signal overlapping region. When a sensor node needs to determine its own location, a request is sent to the location server. The location server calculates the sensor's location, and then sends the result to the requesting sensor node.

A classical cell-based positioning system is centralized. Because communications between a sensor and a location server consume energy, the classical centralized, cell-based method is not suitable for sensor networks. In order to maintain the advantages of cell overlapping that divides the working area into several independent regions, a *distributed* cell-based positioning method is proposed [20]. Each node makes use of the beacon signals which were broadcast periodically from the anchors to estimate its own location. In this paper, we design a distributed multiple power-level, cell-based positioning method for wireless sensor networks.

First, certain beacon frames of the anchor contain the anchor's position, all power-levels, and the power-level of this beacon. A sensor node estimates its position based on the information in the beacon frames. The proposed method is distributed and simple. *Distributed* means that the location is determined by individual sensor node. There is no need for a GPS receiver or a central server. *Simple* means that sensor nodes only use a simple connectivity metric and positioning data in the beacon frames to calculate their own locations. Sensor nodes require little computation. This method is described in the next section.

4. Multiple power-levels positioning method

The signal overlapping technique was used to perform node localization [12]. An extension of the signal overlapping technique with multiple power-level is used in this method. The basic idea of our multiple power-levels positioning method is that each reference node (RN) periodically broadcasts beacon frames that contain its coordinates, coverage radii and current coverage radius. Each power-level of RN has its own coverage radius. A reference node is a special-purpose sensor node which knows its own coordinate and has an unlimited supply of electric power. Sensor nodes (SNs) receive the beacon frames to perform localization autonomously.

The proposed localization algorithm can be broken down into four major steps: (1) initial setup, (2) broadcasting beacon frames, (3) processing beacon frames, and (4) computing a node's location. The first two steps are performed at RNs and the last two steps are performed at SNs. The four steps are presented follows:

Step 1: Initial setup. Reference nodes are randomly deployed in the sensing area and their positions can be obtained in advance. It is assumed that the entire sensing area is jointly covered by all RN's signals. We define that p_i^j is the power-level j of RN i and r_i^j is the coverage radius of power-level p_i^j. In Fig. 1, the coordinates of RNs 1 through 4 are (0,100), (100,100), (0,0), and (100,0), respectively. Each RN has four power-levels with the coverage radii (20, 40, 60, and 80).

Step 2: Broadcasting beacon frames. Reference nodes periodically broadcast beacon frames that contain the coordinates of RN, RN's coverage radii of the multiple power-levels and the coverage radius of the current power-level. The beacon frame $S_{P_i^u}$ from RN i in the uth power-level contains the following data:

$$S_{P_i^u} = \{(x_i, y_i), P_i, p_i^c\},$$

where (x_i, y_i) is the coordinate of RN i, P_i is the set $\{p_i^1, p_i^2, \ldots, p_i^j\}$ of power-levels of RN i, and p_i^c is the current power-level. It is noted that $P_i = \{p_i^1, p_i^2, \ldots, p_i^j\}$ where j is the maximum number of power-levels and p_i^c is an element of P_i. According to the free space propagation model, the transmitted signal power can be translated into the signal coverage radius[21]:

$$P_r(d) = \frac{P_t G_t G_r \lambda^2}{(4\pi)^2 d^2 L}, \quad (1)$$

where P_t is the transmitted signal power. G_t and G_r are the antenna gains of the transmitter and the receiver respectively. L is the system loss, λ is the wavelength, and d is the signal coverage radius. It is common to select $G_t = G_r = 1$ and $L = 1$.

Therefore, the content of the beacon frame with power-levels can be transformed into the coverage radii by Eq. (1). This transformed beacon frame $S_{R_i^u}$ from RN i in the uth power-level, contains the following data:

$$S_{R_i^u} = \{(x_i, y_i), R_i, r_i^c\},$$

where (x_i, y_i) is the coordinate of RN i, R_i is the coverage radius set $\{r_i^1, r_i^2, \ldots, r_i^j\}$ of the multiple power-levels of RN i, and r_i^c is the coverage radius of the current power-level. Note that $R_i = \{r_i^1,$

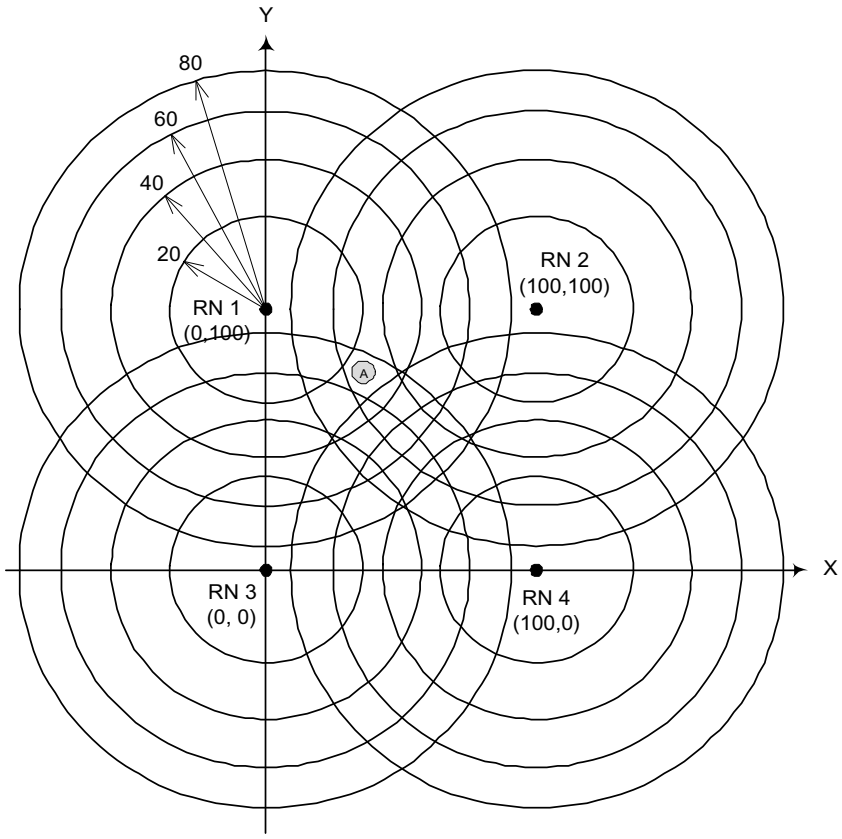

Fig. 1. An example of independent regions for multiple power-levels structure.

$r_i^2, \ldots, r_i^j\}$ where j is the maximum number of power-levels and r_i^c is an element of R_i.

For example, as shown in Fig. 1, RN 1 has four power-levels (i.e. $j = 4$) and periodically broadcasts different beacon frames for each power-level. The contents of the transformed beacon frames for four power-levels are:

In power-level 1: $S_{R_1^1} = \{(0,100),(20,40,60,80), 20\}$.

In power-level 2: $S_{R_1^2} = \{(0,100),(20,40,60,80), 40\}$.

In power-level 3: $S_{R_1^3} = \{(0,100),(20,40,60,80), 60\}$.

In power-level 4: $S_{R_1^4} = \{(0,100),(20,40,60,80), 80\}$.

In this paper, it is assumed assume that the coverage radii of power-levels can be controlled and obtained in the initial stage. Section 4.1 shows how to determine a suitable coverage radius for each power-level.

Step 3: *Processing beacon frames.* After each SN receives enough beacon frames for a short period, it estimates its distance from the RN-based on the minima of the coverage radii of the received beacon frames. Take Fig. 1 for example, the SN *A* receives beacon frames from RN 1. The contents of the transformed beacon frames are as follows:

In power-level 2: $S_{R_1^2} = \{(0,100),(20,40,60,80), 40\}$.

In power-level 3: $S_{R_1^3} = \{(0,100),(20,40,60,80), 60\}$.

In power-level 4: $S_{R_1^4} = \{(0,100),(20,40,60,80), 80\}$.

The SN *A* can obtain the appropriate coverage radius by minimizing the current coverage radii, i.e. Min{40,60,80}=40. According to the coverage radius set and the appropriate coverage radius, the estimated distance from RN 1 to SN *A* is between 20 and 40 units.

Step 4: *Computing a node's location.* After an SN determines its distance ranges from various RNs, the region where this SN may reside can be determined. It is assumed that this SN is located at the centroid of the region. The details of computing a node's location will be discussed in Section 4.2.

4.1. Setting up the optimal coverage radii

An SN's location is determined by the coverage radii of the beacon frames. Intuitively, more and finer-grained coverage radii would result in better estimations at the cost of more delicate electronics in the sensors and more

Table 1
Optimal coverage radii for various numbers of power-levels

Number of power-levels	Optimal coverage radii	Average error
1	(81)	20.0966
2	(62,98)	10.2869
3	(54,79,99)	7.3186
4	(47,69,85,99)	5.8686
5	(37,57,76,89,99)	4.9995
6	(37,54,69,81,91,99)	4.2993
7	(33,48,63,74,83,91,99)	3.714

Table 2
Coverage radii for the first strategy

Number of power-levels	Coverage radii	Average error
1	(99)	31.2008
2	(50,99)	15.2251
3	(33,66,99)	10.5579
4	(25,50,75,99)	8.6427
5	(20,40,60,80,99)	7.1742
6	(17,33,50,66,83,99)	6.0276
7	(14,28,42,57,71,85,99)	5.6187

Table 3
Coverage radii for the second strategy

Number of power-levels	Coverage radii	Average error
1	(99)	31.2008
2	(70,99)	12.9954
3	(57,81,99)	7.8615
4	(49,70,86,99)	6.0703
5	(44,63,77,89,99)	5.2614
6	(40,57,70,81,90,99)	4.4241
7	(37,53,65,75,84,92,99)	3.9646

complicated calculations. According to this experiment, there is little marginal advantage when the number of power-levels exceeds 4.

In Fig. 1, the differences between adjacent coverage radii are always a constant (20). However, this is not necessarily the case, in this experiment, we tried several alternatives.

In this simulation, the working area is a 100×100 square. There is an RN on each of the four corners, and 10,000 sensor nodes are deployed in the square area for each unit distance. These SNs are placed at coordinates $(0,0),(0,1),\ldots,(0,99),(1,0),(1,1),\ldots,(1,99),\ldots,(99,0),(99,1),\ldots,(99,99)$. Positions of sensor nodes are estimated with the proposed localization algorithm and are compared to the actual positions. The average error is a good indication of the overall performance of our localization algorithm. We assume that the area covered by an RN's signal is a circle.

In our simulation, all possible cases of coverage radii of RNs are considered (i.e. using brute force method) and the number of power-levels ranges from 1 to 7. The coverage radii range from 1 to 99. The simulation results are shown in Table 1. As seen, as the number of power-levels increase, the average error decreases. When the number of power-levels exceeds 4, the reduction in the average error is only marginal.

We also used two strategies for testing various coverage radii: (1) the difference of the coverage radii between adjacent power-levels is a constant and (2) the ratio of the coverage radii between power-levels $m+1$ and m is $\sqrt{m+1}$. In the latter strategy, it is easy to verify that the rings between adjacent power-levels cover the same area, as shown in Fig. 2. The simulation results of the two strategies are shown in Tables 2 and 3, respectively. The average errors of Tables 1–3 are plotted in Fig. 3 for comparison. It is obvious that the second strategy (equal-area rings) approaches the optimal coverage radii when the number of power-levels is 4 or larger. In terms of average errors, the second strategy is always better than the first.

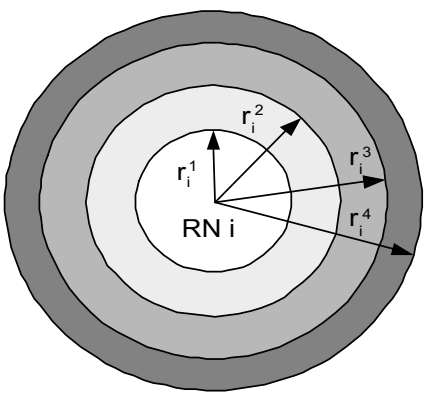

Fig. 2. The equal-area rings.

4.2. Node localization

An SN determines the ring's location from the power-levels of the beacon frames that it can receive from an RN. When receiving multiple RN beacon frames, the SN is located in the overlapping area of the rings. We assume that the SN is at the centroid of the of the overlapping area and the coordinate of it is (x_e,y_e). There are four cases to consider:

Type 1: The sensor node receives beacon frames from only one reference node. In this case, the SN is assumed to be exactly where the RN i is located since the centroid of a ring is the center of the two circles enclosing the ring. (Note that the RN is located at the center of the circles.) The estimated position of SN is:

$$(x_e, y_e) = (x_i, y_i).$$

Take Fig. 4 for example. SN A is located in the ring whose thickness is proportional to r_i^m and r_i^{m+1}, where r_i^m and r_i^{m+1} are the smallest coverage radius and the second smallest coverage radius, respectively, that A can receive from RN i. However, according to this centroid method, the estimated location of A is the centroid of the ring, which is exactly where RN i is located. The error of this estimation is proportional to r_i^m, rather than the difference $r_i^m - r_i^{m+1}$. When r_i^m is large,

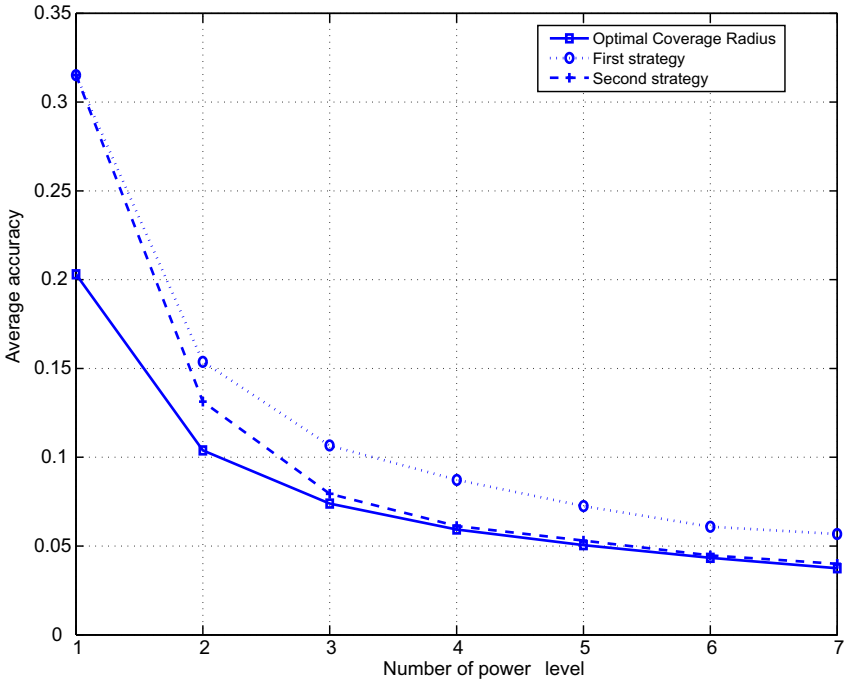

Fig. 3. The average error of optimal coverage radius set, first strategy and second strategy.

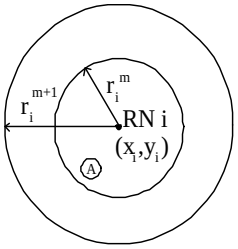

Fig. 4. Type 1 signal overlapping region.

the estimation error could be significant. A possible improvement is to use directional antennae for RNs. However, this solution will incur high cost, power consumption and system complication. In this paper, we only considered an omni-directional antenna for simplicity.

Type 2: The sensor node can receive beacon frames from exactly two reference nodes. Let RNs i and j be the two reference nodes. In this case, the estimated position of SN should be the centroid of the overlapped region of the two rings determined from the strengths of the signals received from RNs i and j. However, computing the exact coordinate of the centroid is too complex a task for a sensor node. An approximation method is used in the following.As shown in Fig. 5, let r_i^m and r_i^n be the least coverage radius that SN can receive beacon frames from RN i and j, respectively. We draw a circle whose center is RN i and whose radius is r_i^m and a similar one around RN j. The intersection of the overlapped region

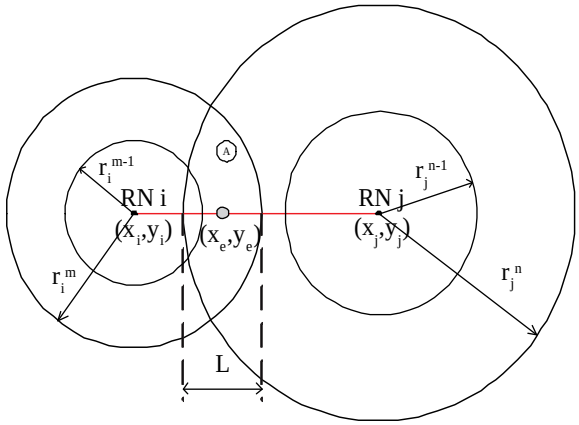

Fig. 5. Type 2 signal overlapping region.

of the two circles and the line linking RNs i and j is a line segment, denoted as L in Fig. 5. The estimated location of the sensor is taken to be the midpoint of the line segment L. Let the coordinates of RNs i and j be (x_i,y_i) and (x_j,y_j), respectively. Let (x_e,y_e) be the coordinate of the midpoint M of L. Thus, we can obtain the following equation:

$$\begin{cases} x_e = x_i + (x_j - x_i)t, \\ y_e = y_i + (y_j - y_i)t. \end{cases} \tag{2}$$

The length of the line segment from RN i to midpoint M is $r_i^m - \frac{L}{2}$. Therefore, we derive the equation:

$$\sqrt{(x_i - x_e)^2 + (y_i - y_e)^2} = r_i^m - \frac{L}{2}. \quad (3)$$

Solving Eqs. (2) and (3), we obtain

$$\begin{aligned}
&\sqrt{(x_i + (x_i - x_j)t - x_i)^2 + (y_i + (y_i - y_j)t - y_j)^2} \\
&= r_i^m - \frac{L}{2} \Rightarrow \sqrt{((x_i - x_j)t)^2 + ((y_i - y_j)t)^2} \\
&= r_i^m - \frac{L}{2} \Rightarrow t\sqrt{(x_i - x_j)^2 + (y_i - y_j)^2} = r_i^m - \frac{L}{2} \\
&\Rightarrow t = \frac{2r_i^m - L}{2\sqrt{(x_i - x_j)^2 + (y_i - y_j)^2}}.
\end{aligned}$$

Let $\overline{ij}$ be $\sqrt{(x_i - x_j)^2 + (y_i - y_j)^2}$. The coordinate of SN, (x_e, y_e), is

$$x_e = x_i + \frac{(x_i - x_j)(r_i^m - r_j^n + \overline{ij})}{2 \times \overline{ij}},$$
$$y_e = y_i + \frac{(y_i - y_j)(r_i^m - r_j^n + \overline{ij})}{2 \times \overline{ij}}.$$

Type 3: The sensor node can receive beacon frames from exactly three reference nodes. As shown in Fig. 6, the position of SN is taken to be the intersection of L_1 and L_2 for the sake of easy computation. In this case, three line segments (L_1, L_2, and L_3) can be obtained, and any two of them can determine the SN's position. To reduce the estimation error, two smallest line segments (L_1 and L_2) are selected. Because a long line segment indicates a large overlapping region of two RNs, it has the higher estimation error. The detailed explanation of this trick will be shown later.

Let i, j, and k be the three reference nodes whose coordinate are (x_i, y_i), (x_j, y_j) and (x_k, y_k), respectively. Let r_i^m, r_j^n, and r_k^o be the least coverage radius of the beacon frames received from RNs i, j, k, respectively. We draw three circles whose centers are RN i, j, and k and whose radii are r_i^m, r_j^n, and r_k^o, respectively. Let I_1 and I_2 be the intersection points of the circles around RNs i and j. Let I_3 and I_4 be the intersection points of the circles around RNs i and k. Let L_1 be the line segment connecting I_1 and I_2. Let L_2 be the line segment connecting I_3 and I_4. The position of SN is taken to be the intersection of L_1 and L_2.

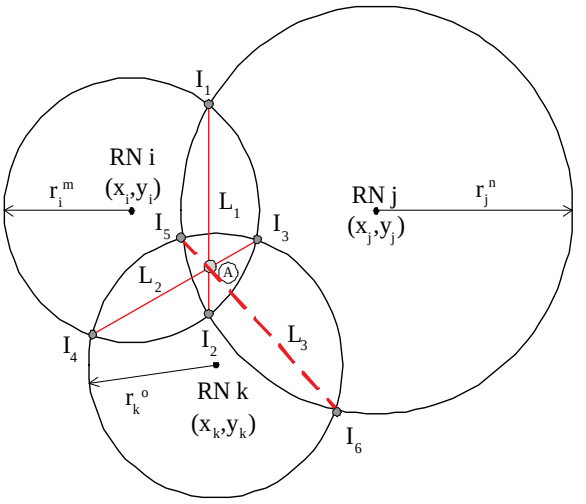

Fig. 6. Type 3 signal overlapping region.

The equations of L_1 and L_2 are

$$\begin{aligned}
L_1 &: (2x_j - 2x_i)x_e + (x_i)^2 - (x_j)^2 + (2y_j - 2y_i)y_e \\
&\quad + (y_i)^2 - (y_j)^2 = (r_i^m)^2 - (r_j^n)^2, \\
L_2 &: (2x_k - 2x_i)x_e + (x_i)^2 - (x_k)^2 + (2y_k - 2y_i)y_e \\
&\quad + (y_i)^2 - (y_k)^2 = (r_i^m)^2 - (r_k^o)^2.
\end{aligned}$$

The coordinate of their intersection can be obtained by solving the above two equations. Therefore, the estimated coordinate of SN, (x_e, y_e), is

$$\begin{aligned}
x_e &= \frac{B_2 * C_1 - B_1 * C_2 + C_1 * D_2 - C_2 * D_1 + C_2 * E_1 - C_1 * E_2}{A_1 * C_2 - A_2 * C_1}, \\
y_e &= \frac{A_2 * B_1 - A_1 * B_2 + A_2 * D_1 - A_1 * D_2 + A_1 * E_2 - A_2 * E_1}{A_1 * C_2 - A_2 * C_1},
\end{aligned}$$

where $A_1 = 2x_j - 2x_i$, $B_1 = (x_i)^2 - (x_j)^2$, $C_1 = 2y_j - 2y_i$, $D_1 = (y_i)^2 - (y_j)^2$, $E_1 = (r_i^m)^2 - (r_j^n)^2$, $A_2 = 2x_k - 2x_i$, $B_2 = (x_i)^2 - (x_k)^2$, $C_2 = 2y_k - 2y_i$, $D_2 = (y_i)^2 - (y_k)^2$, and $E_2 = (r_i^m)^2 - (r_k^o)^2$.

Type 4: The sensor nodes can receive beacon frames from k ($k \geqslant 4$) reference nodes. We first select four "appropriate" RNs among these k RNs and then estimate the sensor node's location based on the four RNs.

(1) *Selection of four appropriate RNs*
Selecting the most "appropriate" RNs is critical to the precision of the estimation. There are two factors that should be considered: First, notice that a smaller overlapped region of the circles around two RNs will result in a

more precise estimation. Take Fig. 7 for example, there are three overlapped regions that are formed by circles around RN i and its three neighbors (j, k, and l). As the overlapped region becomes smaller, the average error tends to decrease. So selecting the pair (i,l) is more plausible than selecting either the pair (i,j) or the pair (i,k).

Second, the intersection of the two lines L_1 and L_2 might fall out of the overlapped region (see Fig. 8). We should be careful that this situation will not occur. On the other hand, if the intersection of every pair of lines falls out of the overlapped region, we will instead choose only a line and consider this as a type-2 case. Thus, we select two RNs, say a and b, among the k RNs to form a line L_{ab} such that $d_{L_{ab}}$ is minimized. Then, we select another two RNs, say c and d, to form line L_{cd} such that $\pi/3 < \theta_{cd} < 2\pi/3$ (where θ_{cd} is defined in the sixth step below). If there is more than one candidate pair (c,d), we will choose the one with the smallest $d_{L_{cd}}$. The algorithm is described as follows.

1. Compute $d_{ij} = \sqrt{(x_i - x_j)^2 + (y_i - y_j)^2}$, for all $i, j = 1,2,\ldots,k$.
2. Compute $d_{L_{ij}} = r_i + r_j - d_{ij}$, for all i, $j = 1,2,\ldots,k$.
3. Find $d_{L_{ab}} = \min\{d_{L_{ij}}\}$.
4. Compute $m_{ab}=(y_a - y_b)/(x_a - x_b)$.
5. Compute $m_{ij}=(y_i - y_j)/(x_i - x_j)$, for all $i = 1,\ldots,k$, $j = i+1,\ldots,k$, $i \neq a$, and $j \neq b$.
6. Compute

$$\theta_{ij} = \cos^{-1}\left(\frac{1 + m_{ab}m_{ij}}{\sqrt{1 + (m_{ab})^2}\sqrt{1 + (m_{ij})^2}}\right)$$

for all $i = 1,\ldots,k, j = i+1,\ldots,k$, $i \neq a$, and $j \neq b$.
7. Choose c and d such that $d_{L_{cd}} = \min\{d_{L_{ij}} \mid \pi/3 < \theta_{ij} < 2\pi/3, L_{ij} \neq L_{ab}\}$. The intersection of L_{ab} and L_{cd} is taken as the estimated location of the SN.
8. If no L_{cd} satisfies the condition in step 7 above, estimate the SN's location with RNs a and b as is done in the above type-2 case.

(2) *Node localization based on four RNs*

As shown in Fig. 9, after four appropriate RNs are selected, the position of SN is taken to be the intersection of L_1 and L_2.

Let i, j, k, and l be the four reference nodes, whose coordinate are (x_i,y_i), (x_j,y_j), (x_k,y_k), and (x_l,y_l), respectively. Let r_i^m, r_j^n, r_k^o, and r_l^s be the least coverage radius of the beacon frames received from RNs i, j, k, l, respectively. We draw four circles whose centers are RN i, j, k, and l and whose radii are r_i^m, r_j^n, r_k^o, and r_l^s, respectively. Let I_1 and I_2 be the intersection points of the circles around RNs i and k. Let I_3 and I_4 be the intersection points of the circles around RNs j and l. Let L_1 be the line segment connecting I_1 and I_2. Let L_2 be the line segment connecting I_3 and I_4. The position of SN is taken to be the intersection of L_1 and L_2. Note that the line segments of L_1 and L_2 are the two smallest line segments.

The equations of L_1 and L_2 are

$$\begin{aligned} L_1 &: (2x_l - 2x_j)x_e + (x_j)^2 - (x_l)^2 \\ &\quad + (2y_l - 2y_j)y_e + (y_j)^2 - (y_l)^2 = (r_j^n)^2 - (r_l^s)^2, \\ L_2 &: (2x_k - 2x_i)x_e + (x_i)^2 - (x_k)^2 \\ &\quad + (2y_k - 2y_i)y_e + (y_i)^2 - (y_k)^2 = (r_i^m)^2 - (r_k^o)^2. \end{aligned}$$

The coordinate of their intersection can be obtained by solving the above two equations. Therefore, the estimated coordinate of SN, (x_e,y_e), is

$$\begin{aligned} x_e &= \frac{B_2 * C_1 - B_1 * C_2 + C_1 * D_2 - C_2 * D_1 + C_2 * E_1 - C_1 * E_2}{A_1 * C_2 - A_2 * C_1}, \\ y_e &= \frac{A_2 * B_1 - A_1 * B_2 + A_2 * D_1 - A_1 * D_2 + A_1 * E_2 - A_2 * E_1}{A_1 * C_2 - A_2 * C_1}, \end{aligned}$$

where $A_3 = 2x_l - 2x_j$, $B_3 = (x_j)^2 - (x_l)^2$, $2y_l - 2y_j i, D_3 = (y_j)^2 - (y_l)^2$, $E_3 = (r_j^n)^2 - (r_l^s)^2$, $A_4 = 2x_k - 2x_i$, $B_4 = (x_i)^2 - (x_k)^2$, $C_4 = 2y_k - 2y_i$, $D_4=(y_i)^2 - (y_k)^2$, and $E_4 = (r_i^m)^2 - (r_k^o)^2$.

Based on the proposed node localization mentioned above, it is possible to estimate the node's position. It is obvious that the estimation error of our method can be improved by using the region of the ring formed by the adjacent coverage radius of an RN or the region formed by some coverage radii. However, the positioning estimation with overlapping ring region will greatly increase the complexity and computational cost. Based on the design philosophy of wireless sensor networks, each sensor node has the restriction of

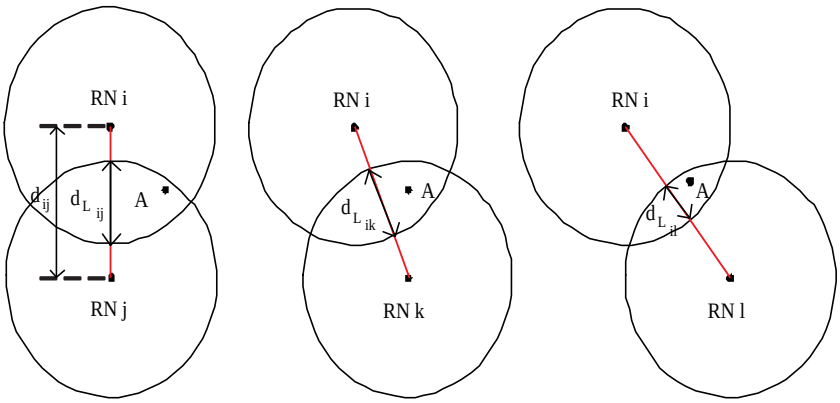

Fig. 7. The effect of average error for different overlapping regions.

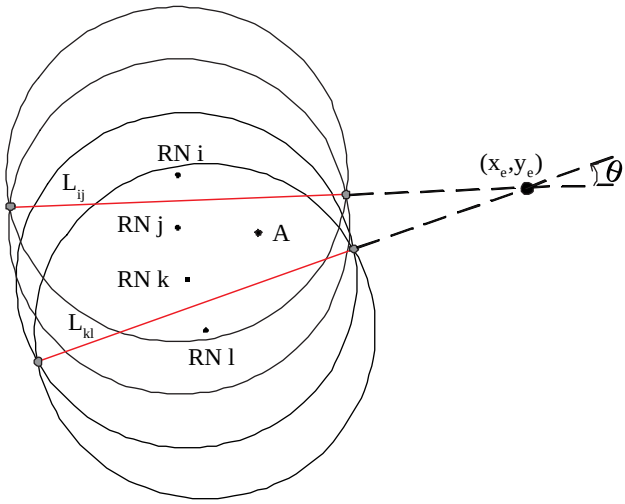

Fig. 8. The estimated location is out of overlapping region.

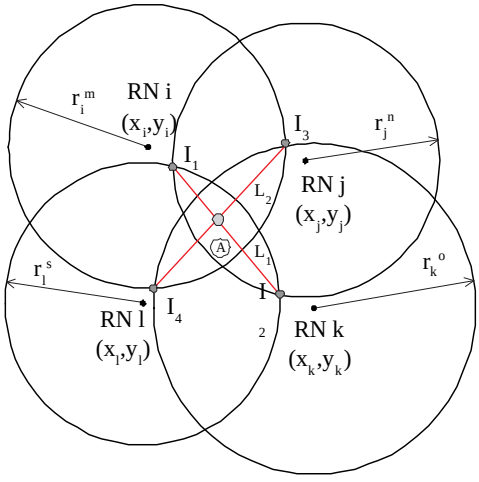

Fig. 9. Type 4 signal overlapping region.

electricity, computational capability and communication bandwidth. A complicated or high computational method is not suitable for wireless sensor networks. Therefore, in this paper, a simple positioning method for wireless sensor networks with acceptable accuracy is considered.

5. Simulation results

In order to evaluate the proposed localization mechanism, we presented several experiments for four situations: failure of RNs, loss of beacon frame, unstable radio propagation model, and random placement of RNs. In addition, we compared our localization mechanism with the range-free positioning method [15] and ad hoc positioning method [16] in terms of computational complexity, communication overhead and average accuracy. Note that for each

Table 4
Simulation parameters

	RN failure	Beacon frame loss	Unstable radio propagation	Random placement of RNs
Power-levels	4	4	4	4
Coverage radii	(47,69,85,99)	(47,69,85,99)	(47,69,85,99)	(47,69,85,99)
Number of RNs	100	4 (at corner)	4 (at corner)	(100,200,300,400,500)
Sensor nodes	10,000	10,000	10,000	10,000
Working area	1000×1000	100×100	100×100	1000×1000
Failure rate	(0%,1%,5%,10%,20%)	0%	0%	0%
Loss rate	0%	(0%,1%,5%,10%,20%)	0%	0%
Propagation model	Ideal	Ideal	Unstable	Ideal
Network structure	Mesh	Mesh	Mesh	Random

experiment, the average error was obtained by 20 runs. The parameters for the experiments are listed in Table 4.

5.1. Reference nodes failure

Reference nodes broadcast beacon frames periodically to provide location information for SNs. In this experiment, we considered the failure rate of RNs in a mesh structure to demonstrate the robustness of the proposed method. Hundred RNs were placed in a mesh structure (i.e. the vertical and horizontal distance between a pair of adjacent RNs were 100) in the 1000×1000 working area. Additionally, 10,000 SNs were also placed in a similar mesh structure in the working area. Should any RNs fail, the estimation error of the locations of nearby SNs could worsen. The maximum error was up to 99 with high RN failure rate. Certain SNs could not even be located (i.e. maximum error = 99) at all because all nearby RNs had failed. Increasing the number of RNs could reduce the number of SNs that cannot be located. The number of SNs that cannot be located and the average error for various RN failure rates are shown in Table 5.

Table 5
The average error for RNs failure

RNs failure (%)	Unlocate SNs	Average error	Maximum error
0	0	5.8686	22.0227
1	2	6.425	77.026
5	66	8.7686	99
10	280	11.917	99
20	1310	18.4823	99

When the RN failure rate was 10%, the number of SNs that could not be located was 280 and the average error was 12 units distance. The defect in the proposed method is in the high failure rate of RNs. Nevertheless, this problem

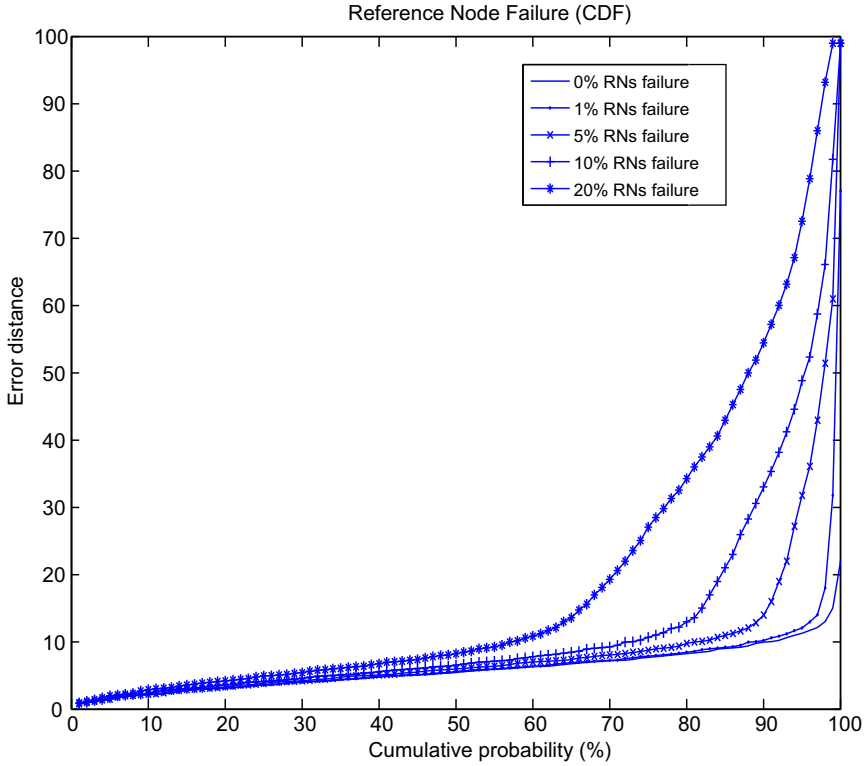

Fig. 10. Error distance CDF for various RNs failure rates.

can be overcome by current hardware manufacturing technology. The cumulative distribution function (CDF) of the error distance is shown in Fig. 10. When the rate was 10%, our method resulted in an 80% error distance to within 15 units distance. According to this experiment, we conclude that the proposed method has high positioning accuracy (low error distance) in low RNs failure rate. In high RN failure rate, there are lots of unlocated SNs since the beacon frames cannot be received by the SNs.

5.2. Beacon frame loss

In a wireless network, a channel can only be used for a single pair of SNs (transmitter and receiver) at any time. Given the limited number of channels, beacon signals are frequently lost due to signal collisions. In this experiment, we studied the effect of beacon frame loss. We tested four beacon frame loss rate: 1%, 5%, 10%, and 20%. There were four RNs, which were deployed in the four corners of the 100×100 mesh area. Table 6 shows the average errors under various beacon frame loss rates. When the beacon frame loss rate was no greater than 5%, the average error increased slightly. When the rate exceeded 5%, the average error became intolerable. As the beacon loss rate became larger than 20%, the maximum error exceeded 90.

Table 6
The average error for beacon loss

Beacon frame loss rate (%)	Average error	Maximum error
0	5.8686	22.0227
1	6.0916	28.6306
5	6.9899	62.8507
10	8.161	54.9281
20	10.6502	94.4299

There are two approaches to reducing the beacon frame loss. One utilizes random backoff or the frequency-division mechanism to reduce beacon collision. The other is for the sensor node to listen for a period of time to collect enough beacon frames. Fig. 11 is the CDF of the error distance relative to the beacon frame loss rate. When the rate was 10%, our method resulted in an 80% error distance to within 15 units distance. Even when the rate was 20%, our method achieved an almost 100% accuracy to within 41 units distance. According to this experiment, it is concluded that the beacon loss rate (less than 20%) slightly affects the average error. It is possibly because the lost beacon frame can be retrieved during another beacon broadcast period.

5.3. Unstable radio propagation model

In reality, the coverage of RNs is irregular due to the multipath propagation effect. In order to evaluate the performance of this method under unstable radio propagation, the shadowing model [21] was considered. The shadowing model can be represented by

$$\left[\frac{P_r(d)}{P_r(d_0)}\right]_{dB} = -10\beta \log\left(\frac{d}{d_0}\right) + X_{dB},$$

where $P_r(d)$ is the power of the received signal at distance d, β is the path loss exponent, and X_{dB} is a Gaussian random

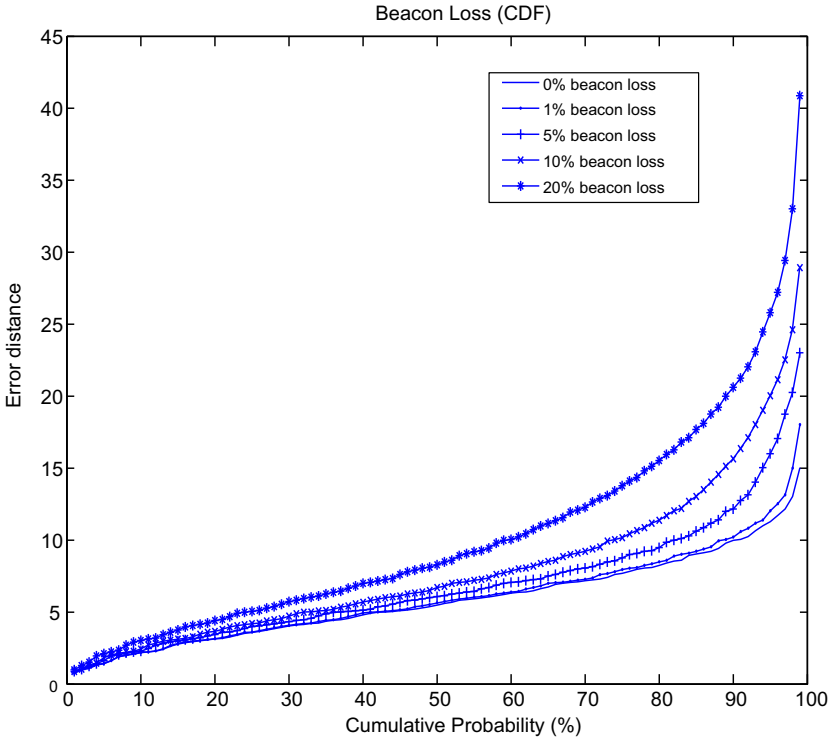

Fig. 11. Error distance CDF relative to beacon frame loss rate.

Table 7
The average error for various σ_{dB} with $\beta = 2$ in shadowing model

σ_{dB}	Average error	Max error
1	6.397	24.5153
2	10.058	50.4385
3	16.7451	78.4235
4	24.0704	86.5351
5	29.9701	93.6641

variable (with $\mu = 0$ and standard deviation σ_{dB}). X_{dB} accounts for the random effect on radio propagation caused by the environment. Note that the shadowing model extends the ideal circle model to a statistic model.

In this experiment, there were four RNs deployed at the four corners of the 100×100 working area. Ten thousand SNs were organized into a mesh, similar to the first experiment. Table 7 shows the average error relative to σ_{dB}. When σ_{dB} was less than 2, the average error was less than 11 and the maximum error was less than 51. This means that this method is applicable in modestly unstable radio propagation environments.

Instability in radio propagation causes a more serious effect in our localization algorithm than do the RN failures and beacon frame losses. The reason for the result is that the shadowing model causes the coverage radius to change as time goes by. The proposed method cannot precisely recognize the localization region of SNs. This means that an SN located in type 1 region might determine its location using the procedure of type 2, 3, or 4 and vice versa. When the mismatch occurred, the error distance of the proposed method became large. Fig. 12 shows the CDF of the error distance in the shadowing model. When σ_{dB} was 3, this method yielded 80% accuracy to within 20 units distance.

5.4. Random placement of reference nodes

The above three simulations only considered the mesh deployment of RNs and SNs. In this simulation, RNs were randomly deployed in a 1000×1000 square area. Table 8 shows the average error relative to the number of deployed RNs. The average error is roughly in inverse proportion to the number of RNs. When the number of RNs was too few, say 100, a significant part of the sensing area was not covered by any RN. Hence, many SNs could not be located (with maximum error = 99). When the number of RNs (say 500) was enough to cover the whole sensing area, all nodes could be located and the average error was only 6.957. The problem of unlocated SNs can be solved by

Table 8
The average error with random placement of RN

Number of RNs	Unlocated SNs	Average error	Maximum error
100	722	30.9267	99
200	80	15.5353	99
300	11	10.0668	99
400	2	8.2485	99
500	0	6.957	67.7213

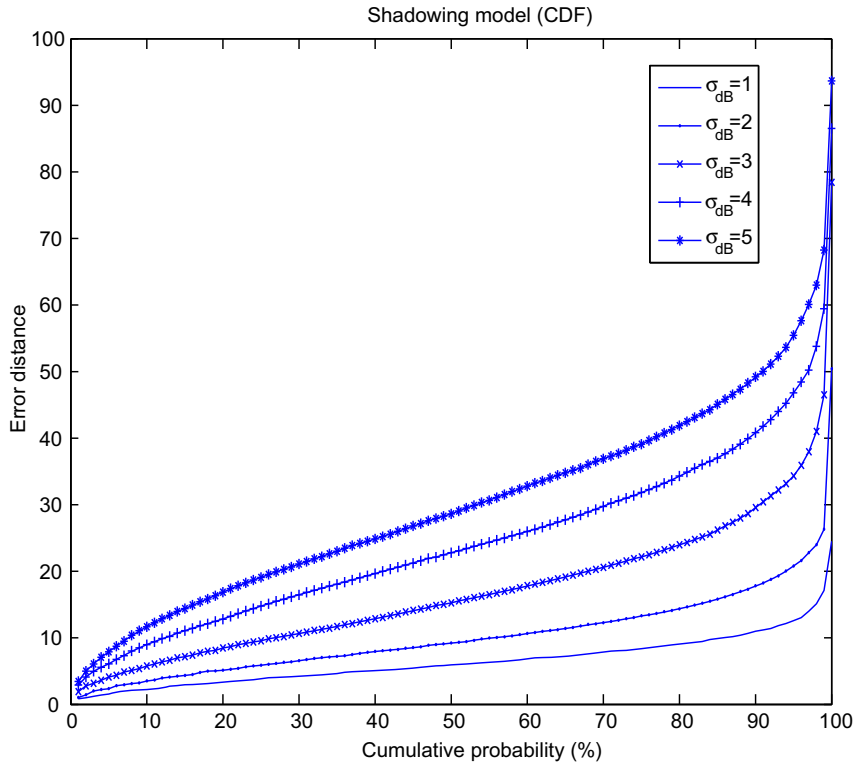

Fig. 12. Error distance CDF for various standard deviation with $\beta = 2$ in shadowing model.

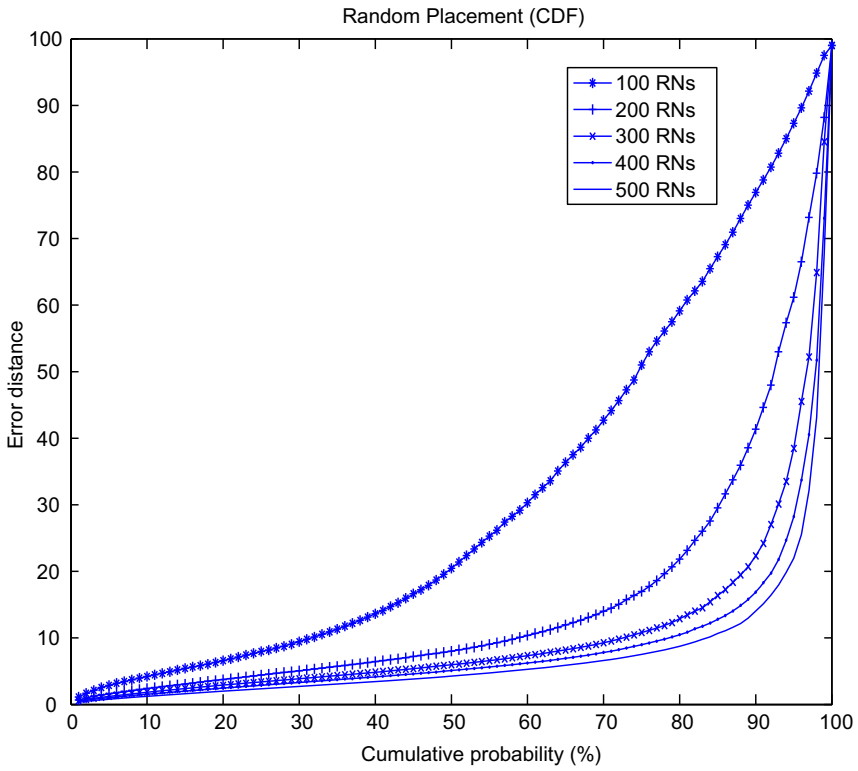

Fig. 13. Error distance CDF for various numbers of RNs with random deployment strategy.

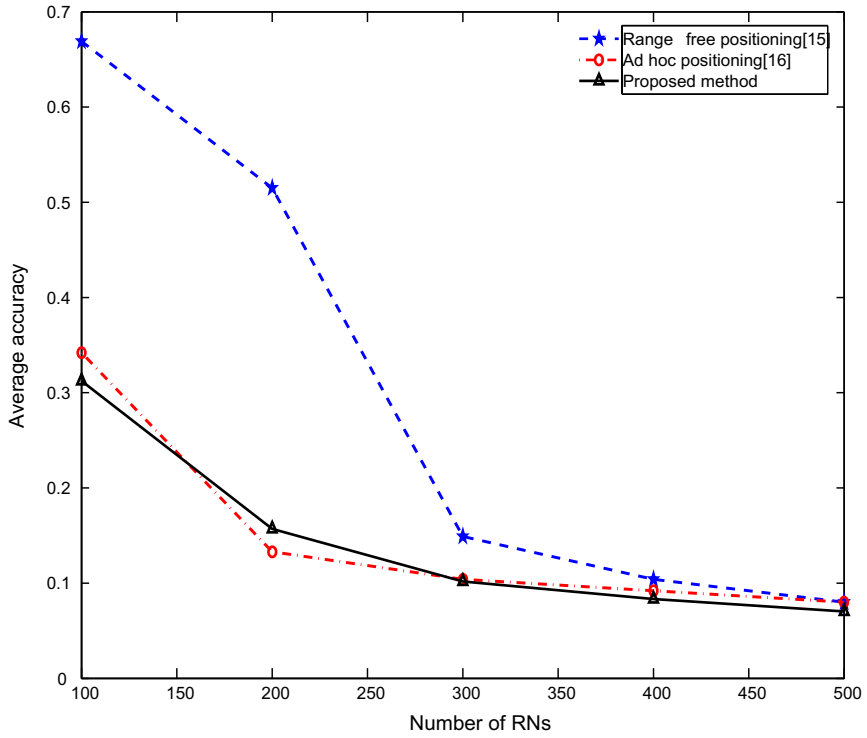

Fig. 14. The average accuracy of range-free positioning [15], ad hoc Positioning [16] and proposed positioning methods for various numbers of RNs.

Table 9
A summary of the system performance and requirement

	Proposed method	APS	Range-free
Total RNs	N	N	N
Beacon transmission	Broadcast	Broadcast	Broadcast
Number of heard RNs	n	n	n
Required RNs	$\geqslant 1$	$\geqslant 3$	$\geqslant 3$
Computational complexity	O(1) (regular)	O(1) (need message exchanging)	$O(n^3)$
	$O(n^2)$ (irregular)		
Communication overhead	No	Yes	No

Table 10
The parameters and hardware information about Mote

Component	Description
Processor	Atmel ATMega 128L
Program flash memory	128K bytes
Configuration EEPROM (Data)	4K bytes
Frequency	868-870 MHz
Radio transceiver	Chipcon CC1000
Battery	2 AA batteries

some possible solutions. One way is to use a density control algorithm to evenly distribute RNs so that the average error can be reduced. Assume that there are n RNs in the sensing field. First, we randomly deploy k RNs in the sensing field where k is a constant and $k < n$ (e.g., $k = n/2$). Find the uncovered region by some existing algorithm. Then, $(n - k)$ RNs are planned for deployment in the place that can totally cover the entire uncovered region. Fig. 13 shows the CDFs of the average error for various numbers of RNs. When the number of RNs was 300, our method gave 80% accuracy to within a 10 unit distance. The reduction in the average error (by increasing RNs) became less obvious when the number of RNs exceeded 300. According to this experiment, it is concluded that as the density of RNs increases, the number of unlocated SNs and the average error both decrease. This is because that lots of beacon frames can be received with high density of RNs.

5.5. Comparison with existing methods

We considered a simulation environment in which RNs were randomly deployed in a 1000×1000 sensing field for various numbers of RNs. In this simulation environment, the average accuracies of range-free positioning method [15], ad hoc positioning (APS) method [16], and our method are compared in Fig. 14. The y-axis is the average accuracy, which is defined as the ratio of the average error distance E_{avg} to the maximum transmission range R_{max} (i.e. E_{avg}/R_{max}, where $R_{max} = 99$).

As shown in Fig. 14, the average accuracy of this proposed method is almost the same as that of the APS method [16] and is much better than that of the range-free positioning method [15]. However, when the number of RNs is more than 300, the average accuracies for the three positioning methods are almost the same.

In Table 9, it shows three important properties. First, all possible signal overlapping regions are classified by the number of heard RNs that is less than four (type 1–4) in our method (i.e. the number of RNs in our method only required at least one RN). In APS and range-free method, at least three RNs are needed to perform the localization algorithm. This property indicates that this method can be employed with fewer RNs. Second, the computational complexity of our method is O(1) when the deployment of RNs is regular. This is because that this method can directly apply the four types of node localization. When the deployment of RNs is irregular, our method should select four appropriate RNs that we mentioned in type 4 (Section 4.2). The first two appropriate RNs are decided by the smallest overlapped region of these two RNs ($O(n^2)$). Then

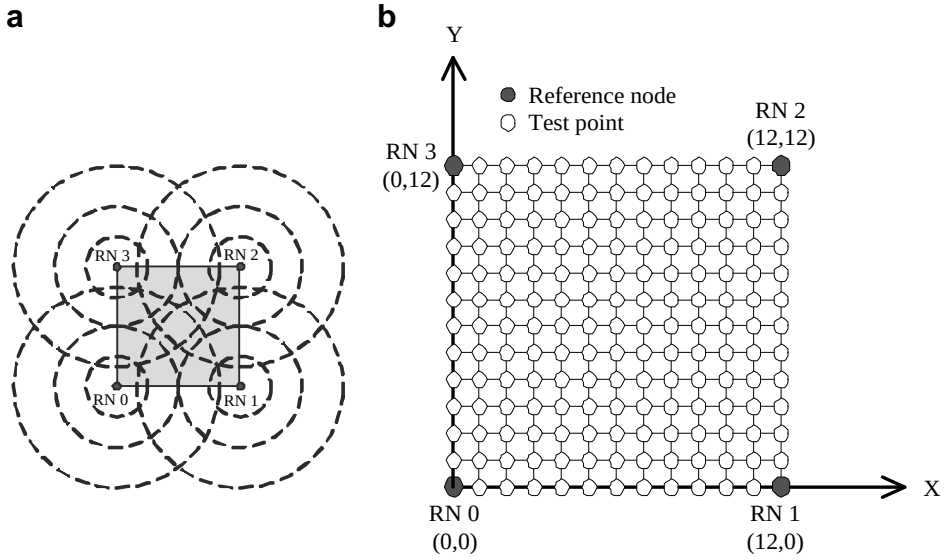

Fig. 15. The topology of RNs.

the last two appropriate RNs can be determined among the remaining of RNs ($O(n^2)$). However, the range-free method makes use of the approximate point-in-triangulation (APIT) test algorithm to find a positioning region. The computational complexity is bounded by $O(N^3)$ since the number of the APIT test is $\binom{n}{3}$. In the APS method, the localization algorithm can be performed immediately by receiving the coordinates and the hop counts of at least three different RNs. Third, the APS method must maintain a table that contains the coordinates and hop counts of RNs and exchange updates with its neighbors. However, with the range-free method and our method these are unneeded. Therefore, the cost of communication overhead and table maintenance in APS method is higher than range-free method and our method. Finally, by considering the computational complexity, communication overhead, and positioning accuracy, our method is more appropriate than either the APS or the range-free method.

Table 11
The beacon content of RNs for three power-levels

RN	Power-level	Beacon content
RN 0	1	{(0,0),(3,6,10),3}
RN 0	2	{(0,0),(3,6,10),6}
RN 0	3	{(0,0),(3,6,10),10}
RN 1	1	{(12,0),(3,6,10),3}
RN 1	2	{(12,0),(3,6,10),6}
RN 1	3	{(12,0),(3,6,10),10}
RN 2	1	{(12,12),(3,6,10),3}
RN 2	2	{(12,12),(3,6,10),6}
RN 2	3	{(12,12),(3,6,10),10}
RN 3	1	{(0,12),(3,6,10),3}
RN 3	2	{(0,12),(3,6,10),6}
RN 3	3	{(0,12),(3,6,10),10}

6. Hardware implementation

The proposed positioning method was implemented over a collection of MICA2 sensor nodes [22] to verify its feasibility and estimate its accuracy in a real-world environment. The resource constraints of MICA2 are listed in Table 10. We placed MICA2 sensor nodes as RNs on an outdoor skating rink in our campus. The topology is shown in Fig. 15(b) in which four black dots represent four RNs. The distance between two adjacent RNs is about 12 m. The transmission power of each RN was tuned so that its transmission range was about 3, 6, and 10 m. Each RN broadcasts a beacon frame every 200 ms. The contents of the beacon frames are listed in Table 11. A white dot with coordinate (x,y), where x and y are integers, in Fig. 15(b) represents a test point. Each time we placed an MICA2 sensor node on a test point (white dot), the sensor node

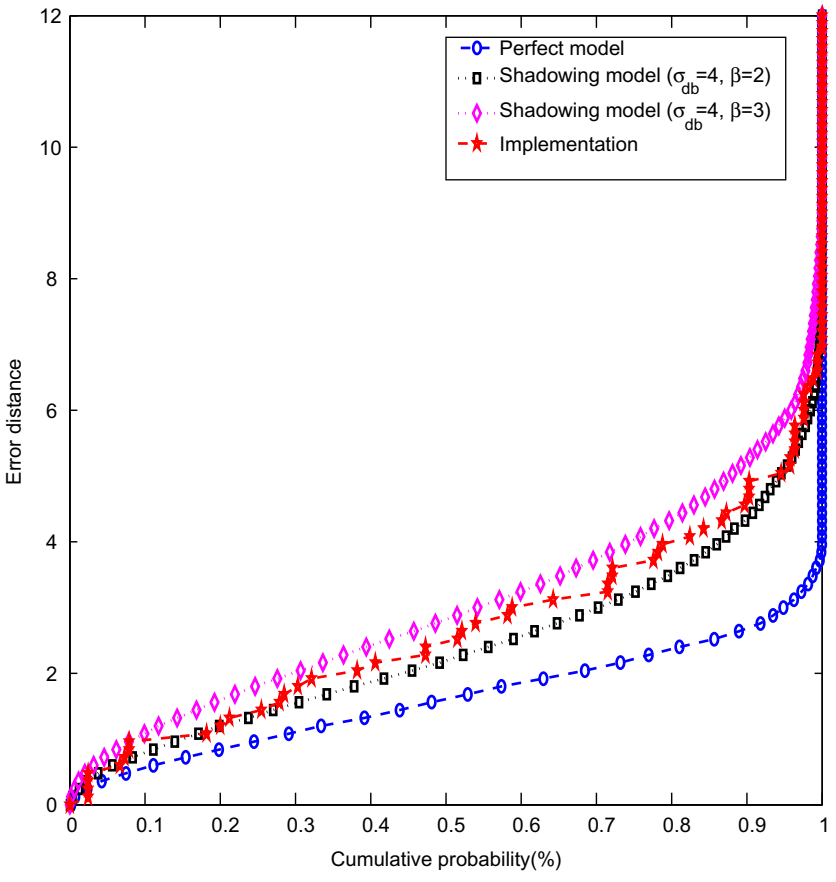

Fig. 16. The average accuracy for hexagonal structure in the experiment.

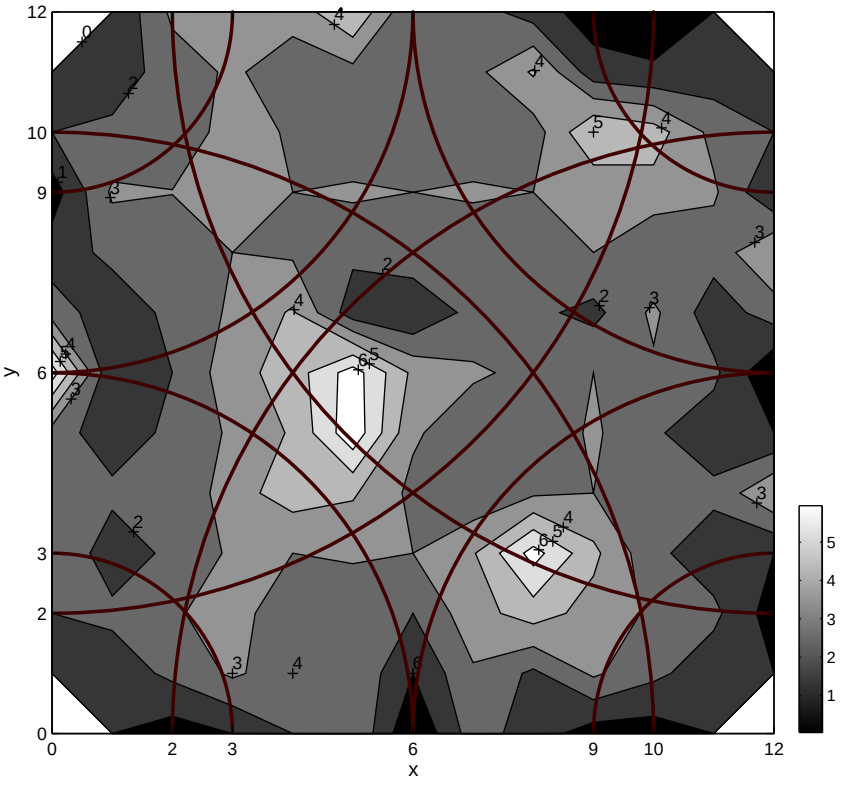

(a) Positioning error.

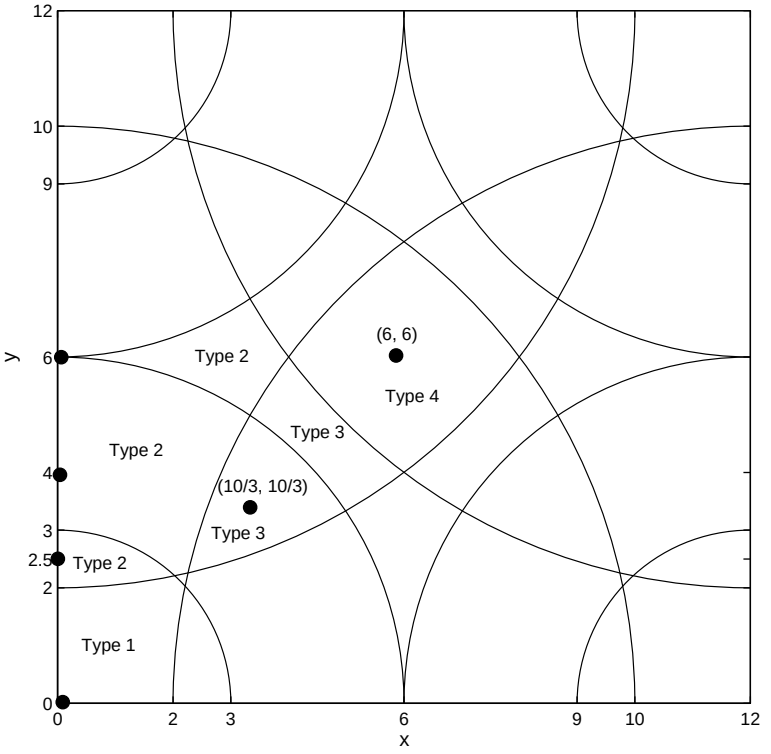

(b) The localization region for type 1 to type 4.

Fig. 17. The positioning error for all test points.

Table 12
The hardware implementation results

x	y	Err	x	y	Err	x	y	Err	x	y	Err	x	y	Err
0	1	1	0	2	2	0	3	3	0	4	2	0	5	2.5
0	6	6.5	0	7	2.5	0	8	1.5	0	9	0.5	0	10	2
0	11	1	1	0	1	1	1	1.41	1	2	2.24	1	3	1.41
1	4	2.24	1	5	1.41	1	6	1	1	7	1.41	1	8	2.24
1	9	3.16	1	10	2.24	1	11	1.41	1	12	1	2	0	0.5
2	1	2.24	2	2	2.83	2	3	2.24	2	4	2	2	5	2.24
2	6	2	2	7	2.24	2	8	2	2	9	3.04	2	10	2.06
2	11	2.5	2	12	3.2	3	0	1	3	1	3.16	3	2	3.61
3	3	3.16	3	4	3.61	3	5	3.16	3	6	3.61	3	7	3.16
3	8	3	3	9	3.04	3	10	3.61	3	11	3.16	3	12	3
4	0	2	4	1	2.43	4	2	2	4	3	3	4	4	4.47
4	5	4.12	4	6	4.47	4	7	4.12	4	8	2.83	4	9	3
4	10	2.83	4	11	2.43	4	12	3.4	5	0	3	5	1	2.87
5	2	2.24	5	3	3.16	5	4	4.12	5	5	6.73	5	6	6.5
5	7	1.41	5	8	2.24	5	9	3.16	5	10	2.24	5	11	2.69
5	12	4.96	6	0	0	6	1	1	6	2	2	6	3	3
6	4	2.75	6	5	3.14	6	6	3.77	6	7	1	6	8	2.75
6	9	3	6	10	2	6	11	2.24	6	12	2	7	0	2.5
7	1	2.87	7	2	3.61	7	3	3.91	7	4	2.24	7	5	2.36
7	6	3.14	7	7	2.36	7	8	2.24	7	9	3.16	7	10	2.24
7	11	2.69	7	12	2.5	8	0	1.5	8	1	1.8	8	2	4.47
8	3	6.4	8	4	2.83	8	5	2.24	8	6	2.75	8	7	2.24
8	8	2.83	8	9	3	8	10	2.5	8	11	4.12	8	12	1.5
9	0	0.5	9	1	3.16	9	2	3.61	9	3	4.24	9	4	3
9	5	3.16	9	6	3	9	7	1.7	9	8	3	9	9	3.16
9	10	5	9	11	1.41	9	12	0.5	10	0	0.5	10	1	2.24
10	2	2.83	10	3	2.24	10	4	2	10	5	2.13	10	6	2.83
10	7	3.2	10	8	2	10	9	3.61	10	10	4.47	10	11	1.12
10	12	0.5	11	0	1	11	1	1.41	11	2	2.24	11	3	1.41
11	4	2.24	11	5	1.41	11	6	2.24	11	7	1.41	11	8	2.43
11	9	3.16	11	10	2.69	11	11	1.41	11	12	1	12	1	1
12	2	0.5	12	3	1	12	4	4	12	5	1	12	6	0
12	7	2.5	12	8	4	12	9	1	12	10	2	12	11	1

collected beacon frames for 9600 ms. Let N_A be the total number of beacon frames collected at test point A and $N_A(i)$ be the number of beacon frames collected at test point A that were issued from RN i. The sensor node at test point A discards the beacon frames from RN i if $\frac{N_A(i)}{N_A}$ is less than 0.1. Based on the beacon frames it collected, the sensor node localized itself by the proposed positioning method. This experiment measured 165 test points as shown in Fig. 15.

Fig. 16 shows the average accuracy for the experimental and simulation results. We use 12 m as a unit distance in our experiment. As shown in Fig. 16, the SN can localize itself to within 5 m for 94.54% of measurements in the outdoor experiments. The experimental results also agree with the simulation results using the shadowing model ($\sigma_{dB} = 4$, $\beta = 3$, and $\beta = 4$). The positioning error obtained from the experiments is plotted in Fig. 17(a) and the localization region with its centroid for type 1–4 is shown in Fig. 17(b). The positioning error is lower for the test points at the centroid of the type 1 regions (at corner). The average positioning error was 2.5 m and the standard deviation was 1.2 m. The minimum error was 0 m and the maximum error was 6.73 m across 165 test points. The implementation result is listed in Table 12.

7. Conclusion

This study presented a multiple power-levels approach to localization for sensor networks. The proposed method is simple, fast, energy-efficient, and requires no additional devices. With four power-levels in an ideal propagation model, the average error is less than 6 units. The robustness of this method was examined under four conditions: reference node failure, beacon frame loss, unstable radio propagation, and random deployment of RNs. Finally, the positioning method was implemented on a sensor network test bed to verify its feasibility. The actual measurements show that it can achieve average accuracy within 0.21 (i.e. $E_{avg}/R_{max} = 2.5/12$) unit in an outdoor environment.

The crux of this method is to utilize multiple power-levels. Many existing algorithms in wireless networks can be enhanced with the technique of multiple power-levels. For example, routing algorithms can make use of multiple power-levels to measure distances between sensor nodes. A sensor could conserve energy by choosing the lowest power-level when communicating with other nodes.

References

[1] I.F. Akyildiz, W. Su, Y. Sankarasubramaniam, E. Cayirci, Wireless sensor networks: A survey, Computer Network 38 (2002) 393–422.
[2] M. Voddiek, L. Wiebking, P. Gulden, J. Wieghardt, C. Hoffmann, P. Heide, Wireless local positioning, IEEE Microwave Magazine 4 (2004) 77–86. December.
[3] J. Hightower, G. Borriello, Location systems for ubiquitous computing, IEEE Computer 34 (8) (2001) 57–66. August.
[4] B. Hofmann-Wellenhof, H. Lichtenegger, J. Collins, Global positioning system: Theory and practice, fourth ed., Springer-Verlag, New York, 1997.

[5] R. Want, A. Hopper, V. Falcao, J. Gibbons, The active badge location system, ACM Transactions on Information Systems (1992) 91–102.
[6] A. Harter, A. Hopper, P. Steggles, A. Ward, P. Webster, The anatomy of a context-aware application, in: Proceedings of the 5th Annual International Conference on Mobile Computing and Networking (Mobicom 99), ACM Press, New York, 1999, pp. 59–68.
[7] N.B. Priyantha, A. Chakraborty, H. Balakrishnan, The cricket location-support system, in: Proceedings of the 6th Annual International Conference on Mobile Computing and Networking (Mobicom 00), ACM Press, New York, 2000, pp. 32–43.
[8] P. Bahl, V.N. Padmanabhan, RADAR: An in-building RF-based user location and tracking system, in: Proceedings of the IEEE Annual Joint Conference on IEEE Computer and Communications Societies (INFOCOM'00), 2000, pp. 775–784.
[9] J. Hightower, R. Want, G. Borriello, SpotON: An indoor 3d location sensing technology based on RF signal strength, UWCSE 2000-02-02, University of Washington, Seattle, February 2000.
[10] G.M. Djuknic, R.E. Richton, Geolocation and assisted GPS, Computer Magazine 34 (2001) 123–125.
[11] L. Doherty, K.S.J. Pister, L.E. Ghaoui, Convex position estimation in wireless sensor networks, in: Proceedings of INFOCOM, vol. 3, 2001, pp. 1655–1663.
[12] H.-C. Chu, R.-H. Jan, A cell-based location-sensing method for wireless networks, Wireless Communication and Mobile Computing 3 (2003) 455–463.
[13] S. Capkun, M. Hamdi, J.P. Hubaux, GPS-free positioning in mobile ad hoc networks, in: Proceedings of the 34th Annual Hawaii International Conference on System Sciences, 2001, pp. 3481–3490.
[14] N. Bulusu, J. Heidemann, D. Estrin, GPS-less low cost outdoor localization for very small devices, IEEE Personal Communications Magazine 7 (5) (2000) 28–34. October.
[15] T. He, C. Huang, B. Blum, J. Stankovic, T. Abdelzaher, Range-free localization schemes in large scale sensor networks, in: Proceedings of the ACM/IEEE 9th Annual International Conference on Mobile Computing and Networking (MobiCom'03), 2003, pp. 81–95.
[16] D. Niculescu, B. Nath, Ad hoc positioning system, in: Proceedings of the IEEE Global Communications Conference (GLOBECOM'01), 2001, pp. 2926–2931.
[17] D. Niculescu, B. Nath, Ad hoc positioning system using AoA, in: Proceedings of the IEEE Joint Conference on IEEE Computer Communications Societies (INFOCOM), March 2003, pp. 1734–1743.
[18] W. Ruml, Y. Shang, Y. Zhang, Location from mere connectivity, in: Proceedings of the 4th ACM International Symposium on Mobile Ad Hoc Networking and Computing (MobiHOC'03), 2003, pp. 201–212.
[19] K.-F. Ssu, C.-H. Ou, H.C. Jiau, Localization with mobile anchor points in wireless sensor networks, IEEE Transactions on Vehicular Technology 54 (3) (2005) 1187–1197. May.
[20] H.-C. Chu, R.-H. Jan, A GPS-less, outdoor, self-positioning method for wireless sensor networks, Ad Hoc Networks 5 (5) (2007) 547–557. July.
[21] T.S. Rappaport, Wireless Communications: Principles and Practice, Prentice-Hall, 1996.
[22] T.M. Mote, <http://www.xbow.com/Products/productsdetails.aspx?sid=72>.

Jen-Yu Fang received the B.S. and M.S. degrees in Computer and Information Science from National Chiao Tung University, Taiwan, in 2002 and 2004, respectively. His research interests include wireless networks, mobile computing and wireless internet.

Hung-Chi Chu received the B.S. and M.S. degrees in Computer Science and Engineering from Tatung University, in 1995 and 1997, respectively and Ph.D. degree in Computer Science from National Chiao-Tung University in 2006. He is currently an Assistant Professor in Department of Information and Communication Engineering, Chaoyang University of Technology. His research interests include wireless networks, wireless sensor networks and artificial intelligence.

Rong-Hong Jan received the B.S. and M.S. degrees in Industrial Engineering, and the Ph.D. degree in Computer Science from National Tsing-Hua University, Taiwan, in 1979, 1983, and 1987, respectively. He joined the Department of Computer and Information Science, National Chiao-Tung University, in 1987, where he is currently a Professor. During 1991–1992, he was a Visiting Associate Professor in the Department of Computer Science, University of Maryland, College Park, MD. His research interests include wireless networks, mobile computing, distributed systems, network reliability, and operations research.

Wuu Yang received the B.S. degree in Information Engineering from National Taiwan University in 1982 and the M.S. and Ph.D. degrees in Computer Science from the University of Wisconsin at Madison in 1987 and 1990, respectively. He joined the Computer Science Department in the National Chiao-Tung University since August 1992, where he is a Professor currently. His current research interests include Java and network security, programming languages and compilers, and attribute grammars.